2014 IEEE International Conference on Robotics & Automation (ICRA)
Hong Kong Convention and Exhibition Center
May 31 - June 7, 2014. Hong Kong, China

3D Assembly of Cellular Structures with Coordinated Manipulation by Rail-guided Multi-microrobotic System *

Huaping Wang*, Tao Yue, Masahiro Nakajima, Masaru Takeuchi, Pei Di, Tao Sun, Qiang Huang and Toshio Fukuda, *Fellow, IEEE*

***Abstract*—3D assembly of cellular structures is important for the fabrication of biological substitute in tissue engineering. In this paper, a novel rail-guided multi-microrobotic system was proposed for the assembly of cellular structure. The cellular 2-dimensional (2D) module was fabricated by UV illumination of the crosslinkable hydrogel. The coordinated manipulation among the micromanipulators was performed with newly designed concentric movement along the rail, which realized the arbitrary change of micromanipulator posture. Through the rotation of the end-effectors around the specimen without swapping out the visual field, the manipulation flexibility was improved. The distance information between the micromanipulator and the module was acquired from vision feedback system and utilized for the automatic pick-up of the microstructure. Through the cooperation among multi-manipulators with hybrid motors, the micromanipulation to assemble the 3D structure with 30 nm operation resolution was achieved. Finally, the rail-guided DeSCom system realized the bottom-up fabrication of cellular vascular-like microtube with vision feedback.**

I. Introduction

Tissue engineering as one of the innovative biomedical technologies has echoed widely concerns for achieving the goals of harvesting human tissues in vitro cultivation. Clinical application of engineered tissues has been realized in several tissues such as skin, cornea and cartilage [1]. However, there are still some challenges on the way to engineer the complex organs like heart, liver and kidney. One of the challenges to fabricate the complex biological substitute is the limitation of achieving thick three-dimension heterogeneous composite tissue with vascular network [2-3]. Vascular network as the extra-matrix of cells in the complex tissue provides the access to delivery oxygen and nutrition [4]. Although the oxygen delivery based on diffusion phenomenon can happen within 100-200 μm, the inability to generate the vascular-like structures thinner than 200 μm still hinder the realization of complex tissue with biological significance [5]. To solve the issue of organ loss and failure radically, the new fabrication method aiming at vascular rich structures needs to be addressed.

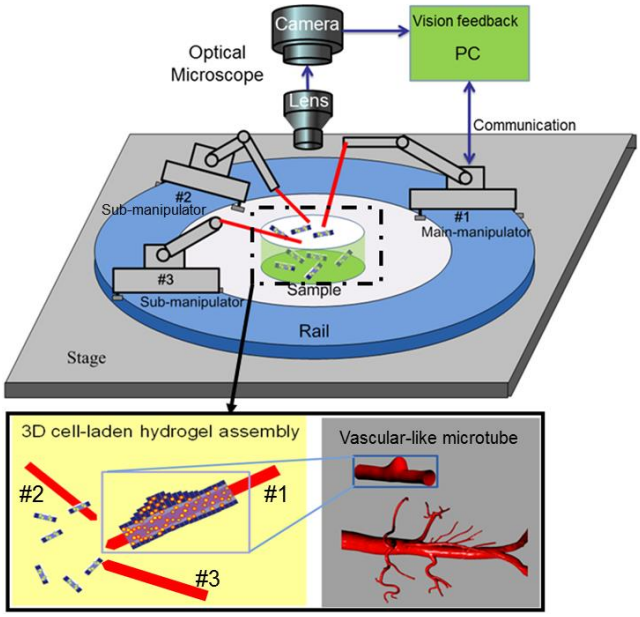

Fig. 1 3D cellular structure assembly with rail-guided DeSCom system

The existing fabrication methods for vascular rich structures are top-down scaffold and bottom-up microfluidic-based system [6]. Scaffolds serving as artificial extracellular matrix provide optimal cellular environments for penetration, ingrowth, and vascularization [7-8]. Through the biodegradation and the growth of the cells at the ratio, the vascular network can be achieved [9]. However, the control of the biodegradation is limited which results the difficulty to fabricate the 3D tissue with micro-scaled structures. From a fluidic point of view, microfluidic systems have emerged as promising tools for building the pathological models of vasculature. Through the assembly of 3-dimensional (3D) cell structure with the precise manipulation provided by optical tweezers, DEP and fluidic forces, the vascular-like structure can be realized [10-12]. However, it is difficult to fully remodeling the native vessel by the fabricated microvasculature incorporating microchannels with rectangle cross-section.

Recently, microrobotic techniques aiming at observation, measurement and immobilization of micro-/nano-scale objects have been developed [13-14]. As one method of bottom-up assembly in generating complex biological tissues,

*Research supported by the National Natural Science Foundation of China under grants 61375108 and 60925014, the National Nature Science Foundation of China for Distinguished Young Scholars under grant 60925014, and "111 Project" under Grant B08043.

Huaping Wang, Tao Sun, Qiang Huang and Toshio Fukuda are with the Intelligent Robotics Institute, Key Laboratory of Biomimetic Robots and Systems, Ministry of Education, Key Laboratory of Intelligent Control and Decision of Complex System, School of Mechatronical Engineering, Beijing Institute of Technology, 5 South Zhongguancun Street, Haidian District, Beijing 100081.

Contacting author: Huaping (phone: +86-68913111; fax: +86-68915812; e-mail: wanghuaping@bit.edu.cn)

Masahiro Nakajima, Tao Yue, Pei Di, Masaru Takeuchi and Toshio Fukuda are with the Institute for Advanced Research, Nagoya University, Nagoya, Japan.

Toshio Fukuda is with the Faculty of Science and Engineering, Meijo University, Nagoya, Japan.

through the direct contact between mechanical end-effector and microstructure without the restriction of operation environment interfering electrically or optically, the microrobotics can provide more stable and flexible manipulation with larger force [15]. For most of the microrobotic systems, the main issue is how to achieve precise control with direct contact during manipulation [16-17]. Researchers have made many achievements in precise robotic manipulation. For example, Hong Qiao proposed the concept of "Attractive Region in Environment" (ARIE) in [18], which is very important in 3D high precision manipulation for manufacturing. In our previous research, the assembly of 3D structure was realized with dual dextrous sticks cooperation. However, the arbitrary change of the tip posture during assembly was not performed [19].

In this paper, we proposed a novel bottom-up assembly method of cellular 3D hydrogel structures based on the rail-guided microrobotic system. To realize the arbitrary change of the end-effector posture during micromanipulation, we amended our previous dextrous sticks coordinated manipulation system (DeSCom) to be the rail-guided DeSCom system. The coordinated manipulation among multi-manipulators was performed with concentric movement along the rail to improve the manipulation flexibility. The 2D microstructure encapsulating cells was fabricated as the assembly module. The vision feedback information was utilized for the movement control and the automatic pick-up of modules with an operation resolution around 30 nm was achieved. The assembly of cellular vascular-like microtube with outer diameter around 200 μm was demonstrated based on the rail-guided DeSCom manipulation.

II. Rail-Guided Microrobotic System for Cellular Structure Assembly

A. Concept

The concept to assemble the cellular structure based on rail-guided system with dextrous stick coordination manipulation is shown in Fig.1. Instead of direct micromanipulation of the cells, cells were encapsulated into biocompatible hydrogel as 2D microstructure for assembly. By creating modular structure, the cell viability during manipulation was assured. Through the integration of different microstructure shapes with the interaction of micromanipulators, the 3D structures with expected morphology can be achieved. To realize the complex structures assembly, the microrobotic system needs to interfere the assembly task in different positions. The tip of the end-effector needs to frequently rotate around the specimen in the visual filed for the adjustment and alignment. The rail-guided system was designed to achieve the arbitrary change of tip posture during manipulation. As shown, the manipulators were restricted on the rail. During the moving of manipulator stage along the rail, the end-effector achieved the concentric motion to rotate the tip around the specimen without sweeping out of the visual field. Considering of assembly efficiency, the image acquired from the optical microscope was utilized for the vision feedback. Through the recognition of different assembly tasks, the cooperation between end-effectors based on image feedback was established. For the sophisticated assembly task in the future, more manipulators as the module can be incorporated into the rail-guided microrobotic system to improve the manipulation flexibility.

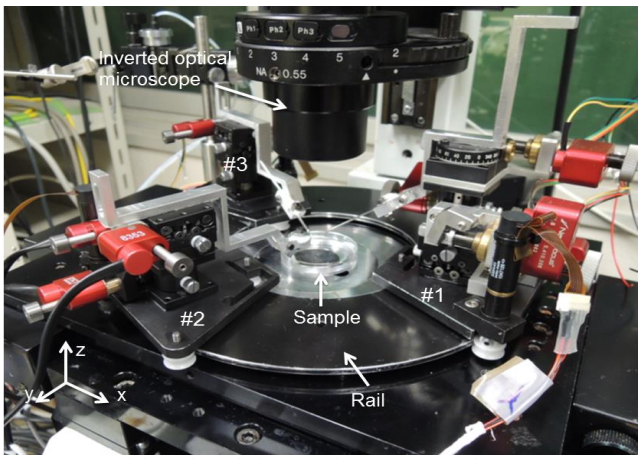

Fig. 2 Setup of the rail-guided microrobotic system under OM

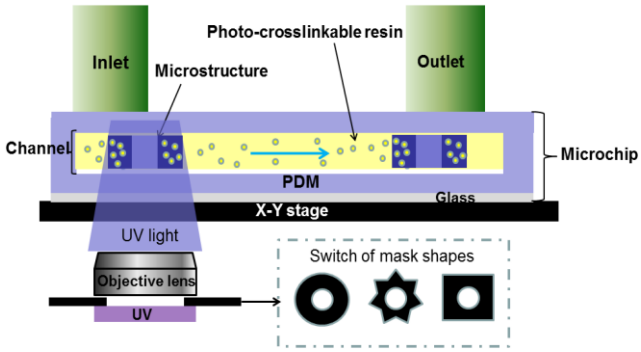

Fig. 3 On-chip fabrication of 2D cellular assembly module

B. Rail-guided microrobotic systems setup

As shown in Fig. 2, we developed the integrated Inverted Optical Microscope (OM)-microrobotic manipulation system to realize the assembly of cellular structure. This system was set up with three sub-systems including the rough control, the fine control and the vision feedback. The manipulator stages were restricted on the rail and driven by the stepping motor (model 398867, Maxon Motor Inc.) for the rough control. Through the concentric movement derived from the stepping motor, the manipulators can move along the rail and the tip of end-effector can rotate around the specimen in the visual field of OM. For every manipulator on the rail, the piezo motor (model 8353, New Focus Inc.) was utilized to realize the fine control. Through the driving of three prismatic joints along X-Y-Z direction respectively, the micromanipulation resolution was around 30 nm. The glass pipette was pulled and sputtered with gold as the end-effector of the micromanipulator and the dimension of the pipette tip is around 10 μm. The vision feedback sub-system was developed to improve the assembly efficiency. Through the processing of image captured from the OM, the distance information was utilized for the target location, task optimization and finally the automatic pick-up of 2D module was achieved.

C. Cellular 2D module fabrication

Instead of direct contact with cells, the cells were encapsulated into the 2D hydrogel modules for the

microrobotic assembly of the 3D cellular structures. The size of assembled structure can be easily regulated through controlling the total number of the 2D hydrogel modules in the assembled array. Through the soft-contact between the hydrogel and the cells, the cell viability during assembly can be assured.

As shown in Fig. 3, we utilize the microfluidic channel to fabricate the 2D modules. The fabrication method is based on the sensitometric characteristic of the crosslinkable hydrogel [20]. After the exposure with UV light, the cell-mixed hydrogel solution can solidify and encapsulate the surrounding cells into the structure. The shape of solidified 2D module is determined by the profile of exposed UV light. To achieve predefined physiological architectures, the UV light source was covered with different masks to shape different profiles of 2D module. Finally, the 2D modules were collected to the buffer solution for the 3D microrobotic assembly.

NIH/3T3 cells as one type of fibroblast forms the outer layer of vessel, so we chose it for 2D module fabrication. The Poly(ethylene glycol) diacrylate (PEGDA, molecular weight 700, Sigma Aldrich) as one type of crosslinkable hydrogel is biocompatible and exhibits mechanical properties similar to those soft tissues, so PEGDA was utilized for the encapsulation of NIH/3T3 cells for 2D module fabrication. Prior to experiment, cells were cultured inside Dulbecco's Modified Eagle's Medium (DMEM, Sigma Aldrich) with 10% Fetal Bovine Serum (FBS, Sigma Aldrich) for 72 hours and mixed inside Phosphate Buffered Saline (PBS, Wako) to form a PBS cell solution of 107/mL cell concentration. The experimental solution was formed by 272 μL PBS cell solution, 120 μL PEGDA, and 8 μL photoinitiator (Irgacure 2959, Ciba). As shown in Fig. 4, after the exposure of UV light to the PEGDA, different shapes of 2D module were solidified and the NIH/3T3 cells were encapsulated in the module. For the assembly of complex architecture, more type of cells can be embedded into different 2D shapes.

III. MICROROBOTIC CONTROL SYSTEM

A. Immobilization method of the 2D hydrogel module

To assemble the 3D structure with rail-guided microrobotic system, the 2D modules were picked up for immobilization, alignment and finally assembled in an array. The pick-up motion is derived from the torque M as in Fig. 5(a). During the press of the glass pipette to the microstructure at contact point, the torque increased through the cooperation among the pressure F_p, friction F_f, gravitational force G and support force F_N. As shown in (1)~(3), to realized the rotation of microstructure with enough torque value, the manipulator just needs to approach the glass pipette in vertical direction with appropriate angle θ to increase the press force. To pick up the microstructure with same thickness, the approaching distance in vertical direction is a constant. As shown in Fig.5(c) and Fig. 5(d), we evaluated the immobilization method through the pick-up of hydrogel donuts with glass pipette. After the calibration of approaching distance, the pick-up success rate can achieve 90%, which is enough for the assembly efficiency.

$$M = (f_1 + F_f)\bullet h + (f_2 + F_N)\bullet \frac{D}{4} \quad (1)$$

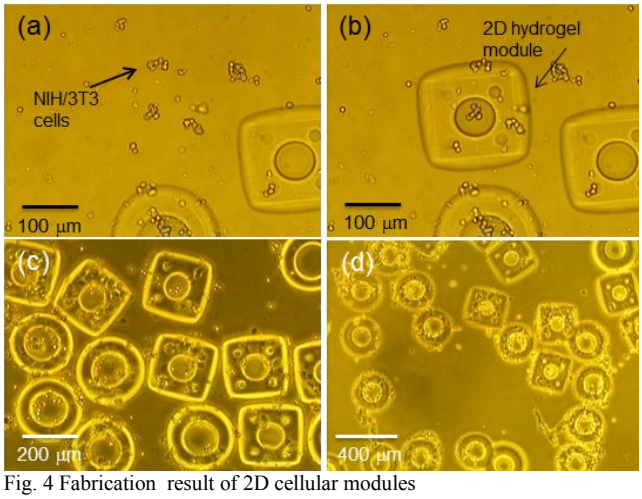

Fig. 4 Fabrication result of 2D cellular modules

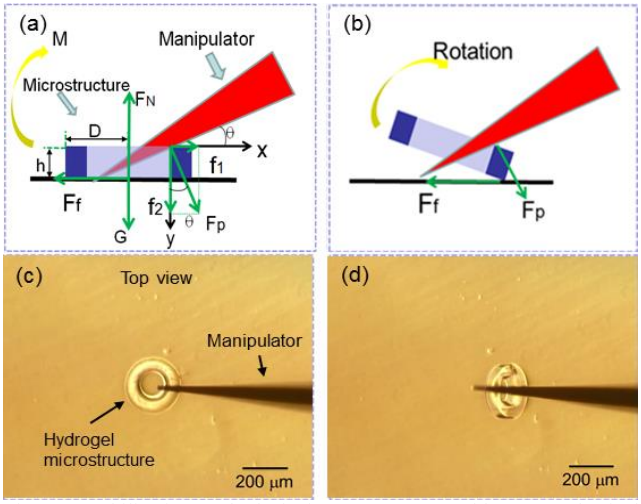

Fig. 5 Immobilization method of microstructure assembly. (a) Mechanical analysis before immobilization. (b) Rotation of microstructure. (c) Experiment evaluation of immobilization method. (d) Rotation of microstructure in the experiment.

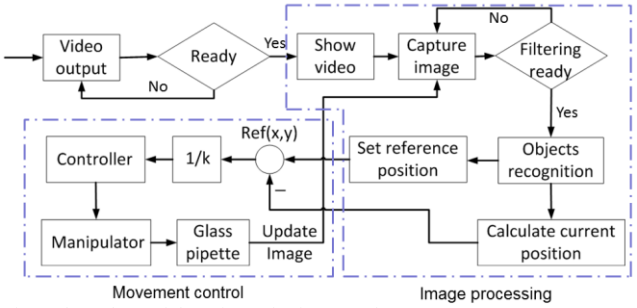

Fig.6 Flow chart of the microrobotic control system

$$f_1 = F_p \bullet \sin\theta \quad (2)$$

$$f_2 = F_p \bullet \cos\theta \quad (3)$$

$$\sum (SCR((x_0 + \Delta x),(y_0 + \Delta y)) - ROI(x_0, y_0)) \quad (4)$$

B. Image processing for Objects Identification

The image captured from OM was utilized as the original image for the vision feedback system. Through the real-time update and processing of image, the distance information was sent back for the movement control of the glass pipette. As

shown in Fig. 6, the feedback control system for 3D structure assembly was based on the image processing. First, the real-time image was captured from OM. Then, the glass pipette and the 2D modules were identified. The target position was set and the current distance was calculated as the movement control feedback. During the movement control, the image was updated and the new distance was calculated again in real-time. Finally, the automatic pick-up of the 2D modules based on microrobotic control system was achieved.

During the image processing, the gray processing and binaryzation processing was utilized to reduce the noise as shown in Fig. 7(a). Based on the Template matching technique in (4), the tip of the glass pipette was taken as the template to identify the glass pipette during manipulation. Fig. 7(c) showed the template matching result where all the tips of pipette were located. Since the shape of 2D module was predefined, the Hough Transformation technique was utilized to identify the 2D modules. As shown in Fig. 7(b), the eligible 2D module which was closest to the main-manipulator was located. The image processing result was shown in Fig. 7(d). The tip point and the center point were defined for distance calibration and movement control. According to the immobilization method, the moving distance in vertical direction was predefined as a constant related to the thickness of the 2D module, so finally the automatic pick-up of 2D module was achieved with image processing.

C. *Glass pipette movement control*

The movement of the micromanipulator was controlled by the stepping motor and piezo motor. As shown in Fig. 8, every micromanipulator configured one revolute joint and three prismatic joints. The frame 0 was fixed on the stage. The frame 1 was fixed on the revolute joint which can achieve the rotate in Z_1 direction derived from the concentric motion of the stepping motor along the rail. The frames 2, 3, 4, were fixed on the prismatic joint which can translate in their Z directions driven by the piezo motors. Frame 5 was the tool frame which fixed on the tip of the glass pipette. The product of all five link transformation matrix can be described according to the Denavit–Hartenberg parameters, which was given by:

$$ {}^{0}_{5}T = {}^{0}_{1}T\,{}^{1}_{2}T\,{}^{2}_{3}T\,{}^{3}_{4}T\,{}^{4}_{5}T = \begin{bmatrix} -\cos\theta_1 & \sin\theta_1 & 0 & p_x \\ -\sin\theta_1 & -\cos\theta_1 & 0 & p_y \\ 0 & 0 & 1 & p_z \\ 0 & 0 & 0 & 1 \end{bmatrix} \tag{5} $$

where

$$ p_x = (R + d_2)\bullet\sin\theta_1 - (d_3 + L_3)\bullet\cos\theta_1 \tag{6} $$

$$ p_y = -(R + d_2)\bullet\cos\theta_1 - (L_3 + d_3)\bullet\sin\theta_1 \tag{7} $$

$$ p_z = L_1 + L_2 + d_4 \tag{8} $$

where L_i (i=1, 2, 3) was the constant height of piezo motor module and d_x (x=1~4) was the translational movement of every prismatic joint which is variable values. R is the radius of the rail. The angle θ_1 was determined by the concentric rotation along the rail. It was a constant during the movement control of the pipette tip, since the posture of the tip was set by the rotation in advance. Thus, the moving of glass pipette in

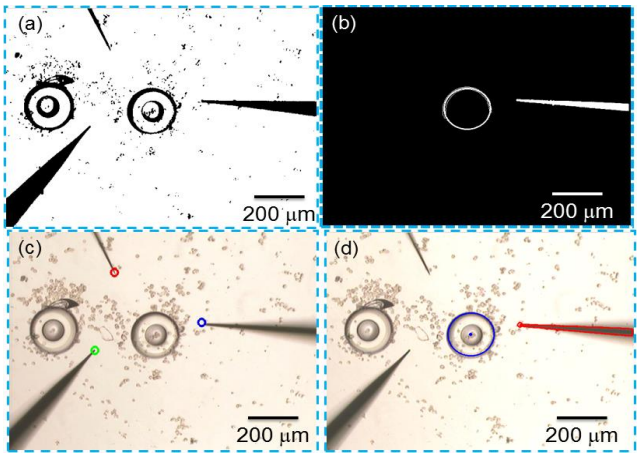

Fig. 7 Image processing result for the rail-guided DeSCom system. (a) Binary image to locate the pipette and the 2D module. (b) Blob image after the filtering. (c) Location image of all tips of the pipette. (d) Result image to set the manipulation start point and end point.

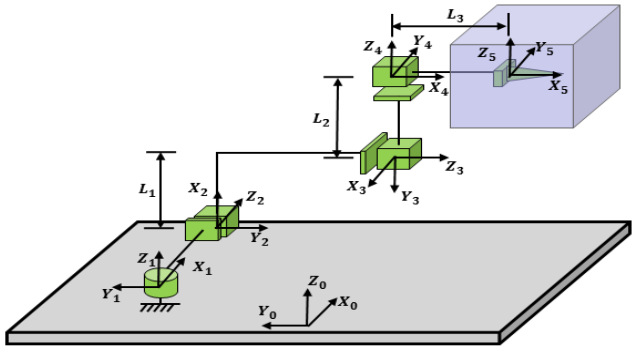

Fig. 8 Kinematic analysis and frame alignments for the manipulator

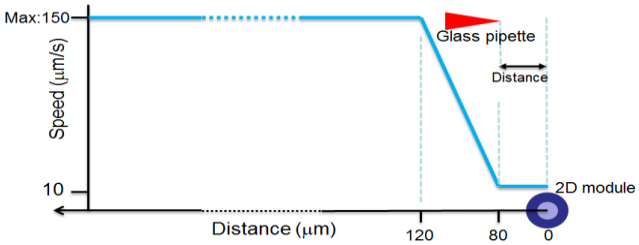

Fig. 9 Movement control based on distance between pipette and 2D module

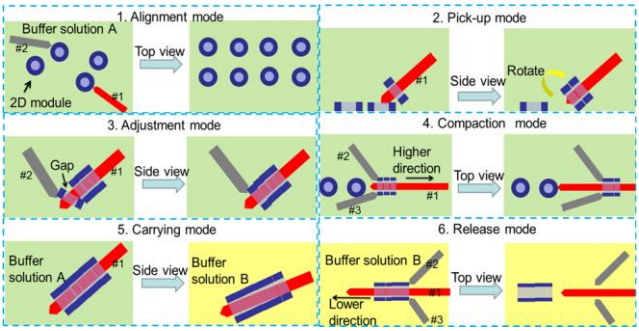

Fig. 10 microrobotic assembly strategies for 3D hydrogel structure

X-Y-Z direction can be easily controlled by the piezo motors respectively. As shown in Fig. 9, the speed control method based on distance was utilized to make the movement control intelligent. The tip of the pipette moved at a maximum speed when the distance to the target donut was long to reduce the movement time. On the contrary, the movement speed

decreased to a relatively lower value to assure the precise when the distance is short.

D. Assembly strategies integration

The assembly of the 2D modules to the 3D structures with rail-guided microrobotic system is a complex task with several manipulation phases. To realize the efficiency and the flexibility during assembly, the manipulation strategies for different phases were designed. Through the utilization of the vision feedback, the mapping between the operation environment and the manipulation strategies can be established, which can realize the automatic choosing of manipulation strategies for different tasks.

As shown in Fig. 10, we designed 6 modes for the assembly of 3D structure. Since the 2D modules were prepared in the solution with different postures, the alignment mode was utilized to qualify the modules and align the qualified modules in an array. After the preparation, the micromanipulator repeated the pick-up mode to gather the modules on the main-manipulator. During the pick-up, the adjustment mode was utilized to adjust the posture of the assembled modules. Through several rounds of pick-up, the compaction mode was used to move the assembled modules to the higher shaft of the pipette with the cooperation between sub-manipulators. After the assembly of enough 2D modules, the assembled 3D structure was carried to new solution for further co-culture. Finally, the release mode realized the release of the 3D structure. Through the image processing, the state of every manipulator was monitored and the automatic switch between different modes were achieved.

IV. Experimental Result

After the design of the vision feedback system for automatic pick-up in the 3D structures assembly and the integration of assembly strategies, we set up the experiment to realize the bottom-up assembly of the cellular vascular-like microtube with the rail-guided microrobotic system.

A. Experiment setup

As shown in Fig. 11, the schematic diagram showed the microrobotic assembly of the cellular microtube with the cooperation between main-manipulator and sub-manipulators. The 2D donuts as the assembly module were prepared in the dish. With vision feedback, the automatic pick-up of the modules was established. Through the monitoring of the assembly state, the microrobotic system switch different strategies to adjust the donut posture and compact the assembled donuts to make more place on the pipette for new donuts. After regulating expected modules on the main-manipulator, the secondary crosslinking was utilized to connect the donut modules as a whole microtube. After changing the buffer solution, the sub-manipulators cooperated to release the microtube from the main-manipulator. The released microtube can be co-culture in the incubator to be the vascular-like tissue.

B. Assembly of cellular vascular-like microtube

In the experiment, we demonstrate the vision-based assembly of the vascular-like microtube with rail-guided microrobotic system. The outer diameter, inner diameter and

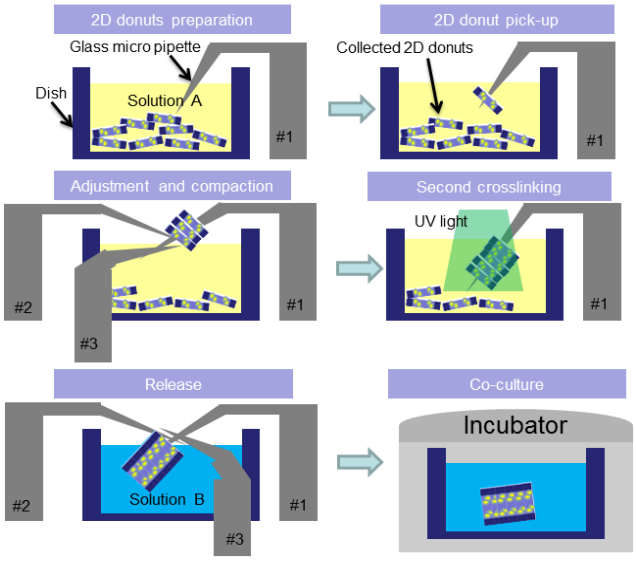

Fig. 11 Experiment setup for the assembly of vascular-like microtube

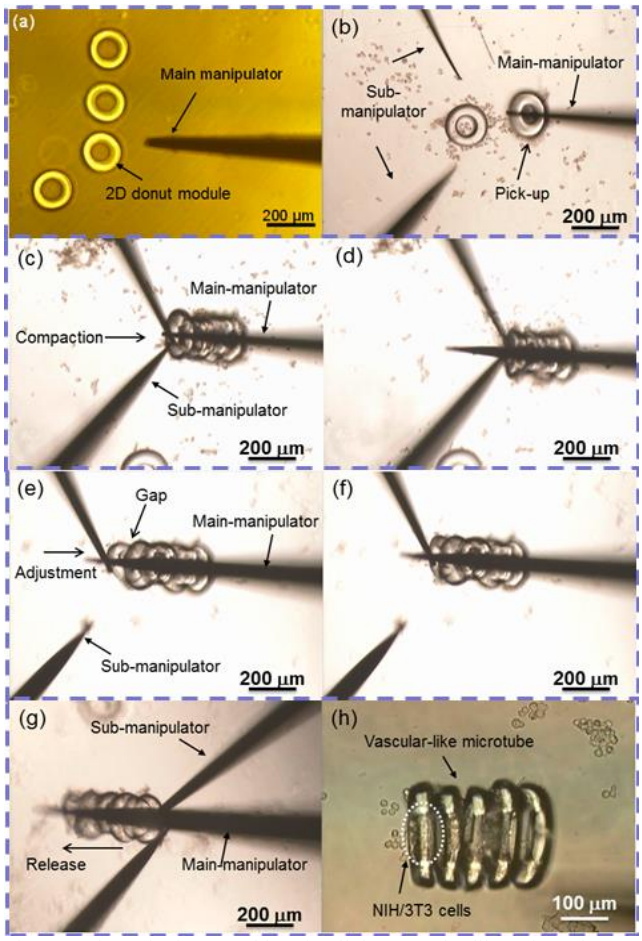

Fig. 12 microrobotic assembly of cellular vascular-like microtube. (a) Alignment of the 2D donuts. (b) Pick-up of donuts. (c), (d) Compaction of assembled donuts. (e), (f) Posture adjustment of assembled donuts. (g) Release of assembled microtube. (h) Release result.

thickness of the fabricated donuts were 200 μm, 100 μm, and 70 μm respectively. During the assembly, the automatic pick-up of the donut was realized according to the glass pipette control method. The distance between the tip of the main-manipulator and the center of the target donut was used

as the feedback in speed control method. As a result, the assembly efficiency and the precision were assured. Besides the automatic pick-up, the image feedback information was also utilized to control the switching of manipulation strategies. As shown in Fig. 12(a), the donuts in the visual field were aligned by the glass pipette as an array. Donuts pick-up was performed once the donuts was aligned. As shown in Fig. 12(b) to Fig. 12(f), during the assembly of donuts, the manipulation strategies were frequently switched from pick-up to adjustment to optimize the posture of assembled donuts, or from pick-up compacting to make new place for more donuts. After the assembly of enough donuts modules and secondary crosslinking, the microtube was finally moved to new culture medium and release from the main-manipulator. As a result, we fabricated a vascular-like microtube encapsulated NIH/3T3 cells inside. The length of the tube is around 350 μm and the diameter is 200 μm.

C. *Discussion*

Fabrication of cellular structures is very important for the tissue engineering. Rail-guided microrobotic system combining with vision feedback allows the automatic fabrication of cellular structures in bottom-up integration way. Through the movement control with image information, the high speed assembly of 2D modules can be achieved. The efficiency and manipulation accuracy were improved. This kind of microrobotic system would benefit the research in biological and medical fields.

In this experiment, we realized the bottom-up fabrication of the vascular-like microstructure encapsulating NIH/3T3 cells inside. The outer diameter of the microtube was around 200 μm, which means that the nutrition and oxygen delivery can happen between the microtubes like the vessel in the tissue. It is meaningful in tissue engineering to fabricate complex biological substitute with vascular network.

Our rail-guided system in this paper achieved the primary work for automatic micromanipulation. Only the target recognition and target approaching in 3 dimensions during pick-up were realized. To achieve the full-automatic micromanipulation, a lot of works like the path planning and control algorithm still need to be considered.

V. CONCLUSION

In this paper, a novel rail-guided micromanipulation system with multi-manipulators cooperation was proposed for the assembly of 3D cellular structures. The 2D hydrogel modules encapsulating cells were fabricated for the assembly. The concentric movement of the micromanipulator to rotate the end-effector around the 2D modules with arbitrary posture was achieved. The real-time OM video was captured as vision feedback for the movement control of the microrobotic system during automatic assembly. The assembly of vascular-like microtube was performed to demonstrate the working mechanism of the automatic system. This rail-guided microrobotic system provides a new concept for high efficient micromanipulation.

ACKNOWLEDGMENT

We thank Hideo MATSUURA at Nagoya University for the help during the mechanism design of the robotic system in the rail-guided DeSCom system.

REFERENCES

[1] L. G. Griffith, G. Naughton, “Tissue engineering – current chanllenges and expanding opportunities”, Science, 2002, vol.295, pp. 1009-1016.

[2] S. A. Hacking, A. Khademhosseini, “Applications of microscale technologies for regenerative dentistry”, Journal of Dental Research, 2009, vol. 88, pp. 409-421.

[3] P. J. Schaner, N. D. Martin, T. N. Tulenko, I. M. Schaner, N. Tarola, R. F. Leichter, R. A. Carabasi and P. J. Dimuzio, “Decellularized vein as a potential scaffold for vascular tissue engineering”, J. Vasc. Surg., 2004, vol. 40, pp. 146-153

[4] L. E. Niklason, J. Gao, W. M. Abbott, K. K. Hirschi, S. Houser, R. Marini and R. Langer, “Functional arteries grown in vitro”, Science, 1999, vol. 284, pp. 489-493.

[5] D. G. Seifu,A. Purnama, K. Mequanint, D. Mantovani, “Small-diameter vascular tissue engineering”, Nature Reviews Cardiology, 2013, vol. 10, pp. 410-421.

[6] J. W. Nichol, A. Khademhosseini, “Modular tissue engineering: engineering biological tissue from the bottom up”, Soft Matter, 2009, vol. 5, pp. 1312-1319.

[7] N. L’Heureux, S. Paquet, R. Labbe, L. Germain and F. A. Auger, “A completely biological tissue-engineered human blood vessel”, FASEB J., 1998, vol. 12, pp. 47-56.

[8] J. T. Borenstein, E.J. Weinberg, B. K. Orrick, C. Sundback, M. R. Kaazempurmofrad, and J. P. Vacanti, “Microfabrication of three-dimensional engineered scaffolds”, *Tissue Engineering*, 2007, vol. 13, pp. 1837-1844.

[9] J. Boublik, H. Park, M. Radisic, E. Tognana, F. Chen, M. Pei, G. Vunjak-Novakovic and L. E. Freed, “Mechanical properties and remodeling of hybrid cardiac constructs made from heart cells, fibrin, and biodegradable, elastomeric knitted fabric”, Tissue Engineering, 2005, vol. 11, pp. 1122-1132.

[10] Y. Wu, D. Sun, W. Huang, and N. Xi, "Dynamics Analysis and Motion Planning for Automated Cell Transportation With Optical Tweezers," IEEE-ASME Transactions on Mechatronics, 2013, vol. 18, pp. 706-713.

[11] T. Yue, M. Nakajima, H. Tajima and Toshio Fukuda, “Fabrication of microstructures and embedding controllable particles inside dielectrophoretic microfluidic devices”, *International Journal of Advanced Robotic Systems*, 2013, vol. 10, pp103-108.

[12] Y. N. Du, M. Ghodousi, H. Qi, et al, “Sequential assembly of cell-laden hydrogel constructs to engineer vascular-like microchannels”, *Biotechnology and Bioengineering*, 2011, vol. 108(7), pp. 1693-1703.

[13] A. Ramadan, K. Inoue, T. Arai and T. Takubo, “Design optimization of a compact 3-DOF parallel micro/nano finger manipulator”, in *Proceedings of the IEEE/RSJ Int. Conf. Intell. Robots Syst.*, 2006, pp. 778-783.

[14] Y. U. Sun, B. J. Nelson, “Microrobotic cell injection”, *Proceedings of the IEEE ICRA*, 2001, pp. 620-625.

[15] L. Dezhong, X. Yihua, and F. Renyuan, “Study of an intelligent micro-manipulator”, J. Mater. Process. Technol., vol. 139, pp. 77-80.

[16] A. Menciassi, A. Eisinberg, I. Izzo, P. Dario, “From “macro” to “micro” manipulation: models and experiments”, IEEE-ASME Transactions on Mechatronics, 2004, vol. 9, pp. 311-320.

[17] A. Ramadan, T. Takubo, K. Oohara, T. Arai, “Developmental process of a chopstick-like hybrid-structure two-fingered micromanipulator hand for 3-D manipulation of microscopic objects”, IEEE Transaction on Industrial Electronics, 2009, vol. 56, pp. 1121-1135.

[18] Hong Qiao and S.K.Tso, “Three-step precise robotic peg-hole insertion with symmetric regular polyhedral objects”, International Journal of Production Research Operation, 1999, vol. 37, pp. 3541-3563.

[19] H. P. Wang, T. Fukuda, et al “Dextrous stick coordination manipulation for 3D hydrogel assembly by dual-nanomanipulator”, Proceedings of the IEEE NANO, 2013, pp. 207-212.

[20] S. E. Chung, W. Park, S. Shin, S. A. Lee, and S. Kwon, "Guided and fluidic self-assembly of microstructures using railed microfluidic channels," Nat Mater, 2008, vol. 7, pp. 581-7.